

Sensitivities to charged-current nonstandard neutrino interactions at DUNE

Pouya Bakhti

School of Physics, Institute for research in fundamental sciences (IPM), PO Box 19395-5531, Tehran, Iran

Amir N. Khan and W. Wang

School of Physics, Sun Yat-Sen University (SYSU), Guangzhou, 510275, China

We investigate the effects of charged-current (CC) nonstandard neutrino interactions (NSIs) at the source and at the detector in the simulated data for the planned Deep Underground Neutrino Experiment (DUNE), while neglecting the neutral-current NSIs at the propagation due to the fact that several solutions have been proposed to resolve the degeneracies posed by neutral-current NSIs while no solution exists for the degeneracies due to the CC NSIs. We study the effects of CC NSIs on the simultaneous measurements of θ_{23} and δ_{CP} in DUNE. The analysis reveals that 3σ C.L. measurement of the correct octant of θ_{23} in the standard mixing scenario is spoiled if the CC NSIs are taken into account. Likewise, the CC NSIs can deteriorate the uncertainty of the δ_{CP} measurement by a factor of two relative to that in the standard oscillation scenario. We also show that the source and the detector CC NSIs can induce a significant amount of fake CP-violation and the CP-conserving case can be excluded by more than 80% C.L. in the presence of fake CP-violation. We further find the potential of DUNE to constrain the relevant CC NSI parameters from the single parameter fits for both neutrino and antineutrino appearance and disappearance channels at both the near and far detectors. The results show that there could be improvement in the current bounds by at least one order of magnitude at the near and far detector of DUNE except a few parameters which remain weaker at the far detector.

I. INTRODUCTION

The discovery of the nonzero value of the neutrino mixing angle θ_{13} has revolutionized the field of neutrino physics in the recent years. This has been made possible after the twenty years long efforts to build and improve the sophisticated detector technology for the measurement of the small value of θ_{13} in the accelerator neutrino experiment, T2K [1] and the reactor neutrino experiments, Double Chooz [2], RENO [3] and Daya Bay [4]. These experiments have measured the value of θ_{13} with unprecedented precision. The next goals in the neutrino oscillation study is to find the correct ordering of the neutrino mass hierarchy (Normal or Inverted), the determination of the CP-violating phase (δ_{CP}), to find the correct octant of the mixing parameter θ_{23} and the precise measurements of all the parameters of the neutrino oscillation scheme. All these unknown parameters and the information will be explored in the medium-baseline reactor neutrino oscillation experiments, JUNO [5] and RENO-50 [6], and in the long baseline accelerator experiments, T2K [7], NO ν A [8], T2HK [9] and the Deep Underground Neutrino Experiment (DUNE) [10].

Two main goals out of the several others in the ongoing DUNE are the measurement of δ_{CP} and determination of the correct octant of θ_{23} . The apparent issue in the simultaneous measurement of these two parameters is their strong correlation with each other. Previously, it has been shown that in $\nu_e/\bar{\nu}_e$ appearance channels, the simultaneous measurement of θ_{23} and δ_{CP} in the long baseline experiments in the region $40^\circ \leq \theta_{23} \leq 50^\circ$ is the better way to measure the two parameters more precisely [11]. The same authors have studied the correlation and their impacts on the measurement of the two parameters by considering both the appearance and disappearance channels at the long baseline experiments, T2HK [12], LBNE [13], IDS-NF [14] and ESS ν SB [15] with different baselines [16]. It has been proven that how the interplay between the two channels can improve the measurements of θ_{23} and δ_{CP} and how the existing degeneracy can be lifted.

In the recent years, after the discovery of the nonzero value of θ_{13} , a wide effort has been put to investigate the hints for NSIs at the neutrino sources and detectors in the reactor short-baseline experiments [17–21] and for the NSIs at propagation in the accelerator long baseline experiments [22–26]. In the latter case, it has been demonstrated recently in Ref. [22] that how the data from DUNE setup can be modified in the presence of different scenarios of NSIs at propagation of magnitude larger than $O(10^{-1})$ if the DUNE data is not consistent with the standard paradigm. There exists degeneracy between the standard mixing parameters and NSI parameters at propagation of the appearance channels in the three long baseline neutrino oscillation experiments T2K, NOVA and DUNE [23]. It was found that at a single L/E_ν , both diagonal and off-diagonal NSI parameters can lead to the four-fold degeneracy that can affect the measurements of mass hierarchy, octant of θ_{23} and δ_{CP} . It was also shown that the degeneracy cannot be resolved even by the combined data of T2K and NO ν A, however a wide-band beam experiment like DUNE can resolve the degeneracy in some scenarios, but not for the others. It was further shown in Ref. [28], that such a degeneracy can also be resolved with the help of a low-energy neutrino oscillation experiment such as MOMENT [29]. Some other

recent work related to the new physics sensitivities at DUNE can be found in Ref. [30–33].

In this work, we consider an alternative approach by considering the charged-current (CC) NSIs which can affect the neutrino production and detection for the case of DUNE. Although neutral-current (NC) NSI which are active during the propagation through the earth matter are more important for the high energy neutrino beams of DUNE, however, the CC NSI at the source and detector are also equally important and cannot be ignored. Since the standard and non-standard NC interactions at the propagation in matter depend on the neutrino energy [34], therefore by combining DUNE, which is a high energy neutrino experiment, with another low energy neutrino experiment such as MOMENT, the degeneracies posed by the NC NSIs to the determination of oscillation parameters can be resolved. However, if the degeneracies produced are due to the CC NSIs, then they cannot be resolved in this way, (see Ref. [28] for details). Moreover, for the near detector only the CC NSIs are relevant while the NC NSIs play no role at the near detector of DUNE, therefore we include the near detector simulated data in addition to far detector. From the near detector alone, we obtain stronger bounds than the existing bounds on the CC NSI parameters as given in the 3rd column of Table I for the 3+3 years of DUNE run. It is also important to note that in future if the DUNE near detector data is combined with the other short-baseline low energy experiments, they will constrain the CC NSI parameters up to several orders of magnitude.

In this work, first we analyze the low-level information at the probability and at the event rate spectrum level and then perform the full statistical analysis to find the sensitivity of DUNE measurements to the CC NSIs at the source and at the detector. We explore the correlation between the two standard parameters θ_{23} and δ_{CP} in the presence of CC NSIs. Analysis with the same goals, but for the different baseline at the ESSνSB facility [15] has been carried out in Ref. [35], where it has been shown that the precision of θ_{23} is robust in the presence of source and detector NSIs, but δ_{CP} measurement gets worsen. Ref. [27]¹ also studies the effects of NC and CC NSI at DUNE in a different perspective, where they consider only the far detector in their analysis and follow an unrealistic approach by considering different NSI at the source and detector. Contrary to Ref. [27], we use the simulated data from both the near and far detectors with equal emphasis on both and taking the advantage of the fact that the NSI at production and detection are the same. We find the effects of the CP-violation caused by NSI phases when the standard $\delta_{CP} = 0$; we called it the fake CP-violation and denote it by δ'_{CP} . Further, we explore the potential of DUNE to constrain the CC NSI parameters at the neutrino source and at the near and far detector and compare them with the current bounds.

This paper is organized as follows. In section II, we present the CC effective four-Fermion NSI Lagrangian and discuss the effects of NSI on oscillation probability. In section III, we discuss about the characteristics of DUNE. The details of our analysis and the results are presented in section IV. The summary and conclusions to this work are given in section V.

II. THEORETICAL FRAMEWORK

For the DUNE set up, high energy beams (up to 10GeV) of neutrino and antineutrinos are produced at the accelerator as a result of pion decays ($\pi^- \rightarrow \mu^- + \bar{\nu}_\alpha$ and $\pi^+ \rightarrow \mu^+ + \nu_\alpha$). They travel over a distances of 1300 km towards the DUNE far detector and over a distance of 450m towards the DUNE near detector and their detection is made through inverse beta decays ($\nu_\alpha n \rightarrow pe^-$ and $\bar{\nu}_\alpha p \rightarrow ne^+$) in the liquid argon scintillation detector. The left-handed four-Fermion CC effective NSI Lagrangian which governs the pion decays at the source and the inverse beta decays at the detectors are given by [17–19]

$$\mathcal{L}_{SM+NSIs} = -2\sqrt{2}G_F(\delta_{\alpha\beta} + \epsilon_{\alpha\beta}^{udL})(\bar{l}_\alpha \gamma_\lambda P_L U_{\beta a} \nu_a)(\bar{d} \gamma^\lambda P_L u)^\dagger + h.c., \quad (1)$$

where α, β are the flavor indices and a is the mass index and all the repeated indices are summed over. We have restricted ourselves to the case of left-handed neutrino helicity and vector and axial-vector quark currents. For simplicity, we do not consider any right-handed NSI couplings. The coefficients $\epsilon_{\alpha\beta}^{udL}$, which are complex in general, are the relative coupling strengths of the different flavor combinations of NSI to the standard model semileptonic, while in the SM case $\epsilon_{\alpha\beta}^{udL} = 0$. Here U is the standard leptonic mixing matrix, parametrized in the standard form. For brevity, we denote all NSI parameters ($\epsilon_{\alpha\beta}^{udL}$) at source and detector by $\epsilon_{\alpha\beta}^s$ and $\epsilon_{\alpha\beta}^d$ where the indices 's' and 'd' stand for the 'source' and 'detector'. Since the production and detection of the neutrinos have the same interaction process at the quark level, we can take $\epsilon_{\alpha\beta}^s = \epsilon_{\alpha\beta}^{d*}$ for the neutrino and for $\epsilon_{\alpha\beta}^d = \epsilon_{\alpha\beta}^{s*}$ for the antineutrino beams and thus

¹ This paper was submitted to arXiv one day before our work.

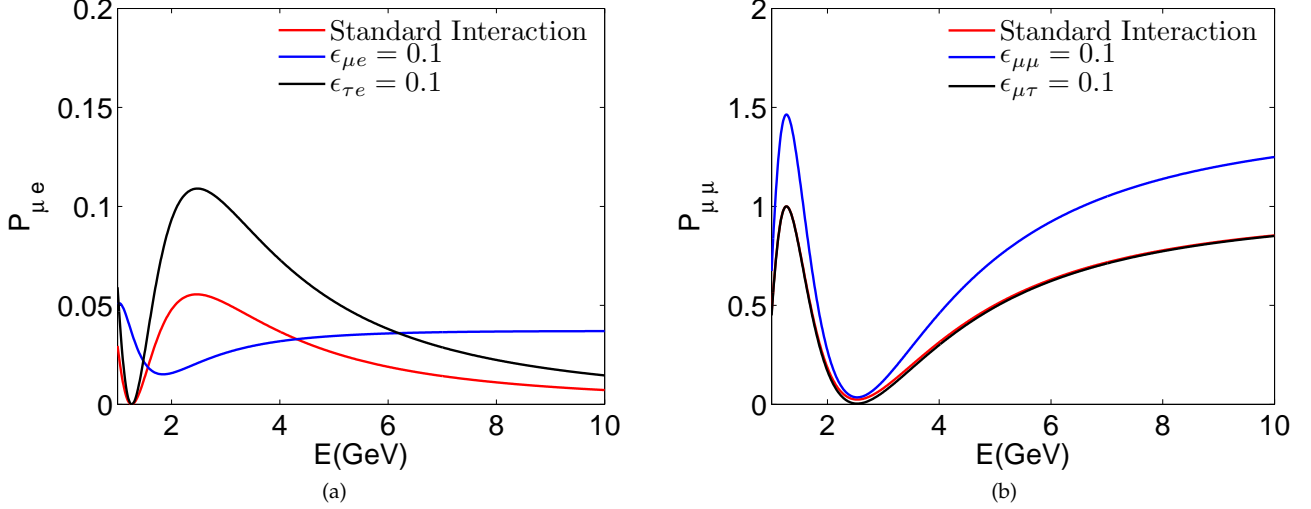


FIG. 1: An illustration of oscillation probabilities at far detector of baseline 1300km for muon neutrino disappearance and electron neutrino appearance. The standard oscillation parameters are taken from nu-fit [40, 41] and $\delta_{CP} = 0$. For NSIs curve, only value of one NSI parameters considered to be nonzero and equal to 0.1. The value of all the phases are set equal to zero.

remove "s" and "d" indices further and denote all the parameters by $\epsilon_{\alpha\beta}$ in general. This pragmatic choice reduces the number of NSI parameters to a half and as a result give better parameter fits. This fact has not been considered in ref. [27] and therefore they get weaker constraints as compared ours on the NSI parameters. Here for $\alpha = \beta$ in the Eq. (1), the summation corresponds to the SM and non-universal flavor diagonal NSI while $\alpha \neq \beta$ corresponds to the flavor-violating NSI.

Channel	standard parameters (FD)	CC-NSI parameters (FD)	CC-NSI parameters (ND)
$P(\nu_\mu(\bar{\nu}_\mu) \rightarrow \nu_e(\bar{\nu}_e))$	$\theta_{23}, \theta_{12}, \theta_{13}, \Delta m_{31}^2, \Delta m_{21}^2, \delta_{CP}$	$\epsilon_{\mu e}, \epsilon_{\tau e}$	$\epsilon_{\mu e}$
$P(\nu_\mu(\bar{\nu}_\mu) \rightarrow \nu_\mu(\bar{\nu}_\mu))$	$\theta_{23}, \Delta m_{31}^2$	$\epsilon_{\mu\mu}, \epsilon_{\mu\tau}, \epsilon_{\tau\mu}, \epsilon_{e\mu}$	$\epsilon_{\mu\mu}$
$P(\nu_e(\bar{\nu}_e) \rightarrow \nu_e(\bar{\nu}_e))$	—	—	ϵ_{ee}

TABLE I: Standard oscillation and NSI parameters that the near and far detectors are sensitive to them for appearance and disappearance channels. Notice the near detector is not sensitive to the standard oscillation parameters.

In our simulation we used GLoBES, and for including the NSI we used oscillation probability formulas from Ref. [36, 37], so we do not repeat the lengthy analytical probability formulas which were calculated using perturbative expansions upto the leading order in the NSI parameters, however we summarize the probabilities and their NSI parameters dependences in table I. In case of the near detector, the baseline $L=0$, therefore the oscillation probability at the near detector does not depend on standard oscillation parameters, and for electron appearance, it depends on $\epsilon_{\mu e}$ and for disappearance mode, it depends on $\epsilon_{\mu\mu}$ and ϵ_{ee} as shown in TABLE I. At the far detector, muon disappearance probability depends on standard oscillation parameters θ_{23} and Δm_{31}^2 and NSI parameters $\epsilon_{\mu\mu}$, $\epsilon_{\mu\tau}$, $\epsilon_{\tau\mu}$ and $\epsilon_{e\mu}$. Electron appearance probability at the far detector depends on all the standard oscillation parameters θ_{23} , θ_{12} , θ_{13} , Δm_{31}^2 , Δm_{21}^2 and δ_{CP} and also on NSI parameters $\epsilon_{\mu e}$ and $\epsilon_{\tau e}$. Dependence of the appearance and disappearance probabilities to the standard oscillation and NSI parameters are listed in table I. For the complete approximate analytical expression of all the oscillation probabilities formulas see Ref. [36].

As a first exercise to see the effects of CC NSIs on the oscillation probabilities at the far detector of the DUNE with baseline of 1300 km are shown in Fig. 1. In Fig 1(a) the electron neutrino appearance probability is shown for the standard interaction and NSIs when only one of the NSI parameters is nonzero and is equal to 0.1. In Fig. 1(b) the disappearance of the muon neutrino is shown. Notice that the values for the standard oscillation parameters and their uncertainties were taken from nu-fit [40, 41] with $\delta_{CP} = 0$ and the resolution of the plot along the energy axis was taken as 0.1 MeV.

III. CHARACTERISTICS OF DUNE AND THE ANALYSIS DETAILS

The DUNE will be a long baseline accelerator based neutrino oscillation experiment where neutrinos/antineutrino beams will be produced at FermiLab and will be detected at Sanford Underground Research Facility, 1300 km away from the FermiLab. In our simulations, we consider 1.2 MW proton beam which produces the neutrino and antineutrino beam from pion decays with the neutrino energy ranging from 100 MeV to 20 GeV and with the peak around 3 GeV. We take the spectrum from Ref. [39] and consider the reference beams for the near and far detector in neutrino and antineutrino modes with 3 years of data taking in each mode. We consider a Liquid Argon Time-Projection Chamber (LArTPC) with 34 kton fiducial mass for the far detector. The details of the near detector are under discussions, however, we consider a near detector with 5 ton fiducial mass placed at 460 m baseline. The NC events, lepton flavor misidentification and the intrinsic background are considered as the main sources of background, while neglecting the other background sources.

We consider the energy resolutions for the CC detections as $15\%/\sqrt{E(\text{GeV})}$ for ν_e and $20\%/\sqrt{E(\text{GeV})}$ for ν_μ , while the efficiency of CC detection of ν_e and ν_μ as 80% and 85%, respectively. Both the NC and Lepton flavor misidentification rates are taken 1%. The flux uncertainty is taken 5%, the calibration error is 2% and the flux uncertainty of the background is 10%. We take the detector performance from Table 4.2 of Ref. [38]. For the analysis, we consider the energy range between 0.25 GeV to 8 GeV and 31 bins in the unit steps of 0.25 GeV. The CC and NC cross sections are taken from Refs. [49, 50]. The number of events in each bin for the standard three neutrino oscillation and in the case of NSI for $\varepsilon_{\mu e} = 0.1$ and $\varepsilon_{\mu\mu} = 0.1$ in the appearance channel and with $\varepsilon_{\mu\mu} = 0.1$ and $\varepsilon_{\tau e} = 0.1$ in the disappearance channel for the near and far detector data are shown in Fig. 2, where the contribution in each bin is the aggregate of both signal and background events. In the near detector appearance mode, almost all of the events are background events since the number of events of the signal is negligible. The values with their uncertainties of the oscillation parameters are taken from nu-fit [40, 41] and the value of the CP phase is taken zero. For matter density profile, we use PREM with 5% uncertainties [46]. Our number of events for near and far detector are in agreement with the result of Refs. [22, 42], except for the slight differences which occur due to the differences in the neutrino fluxes, details of the detector performance, oscillation parameters such as the different value of δ_{CP} . For the result of the near detector, in comparison with Ref. [42], we consider baseline of the near detector equal to 460 m, while they consider 595 m. Moreover, our number of events include both signal and background while they consider only the signal. For simulation and statistical inference, we used GLOBES software [47, 48]. The chi-squared test is used by GLOBES for statistical inferences and a Gaussian error is implied by the software. For considering the CC NSIs, we include the code from Refs. [36, 37]. We consider the uncertainties of source and detector CC NSIs from Ref. [43].

IV. RESULTS AND DISCUSSION

In this section we discuss the main results of the effects of CC NSIs on the determination of the standard parameters, δ_{CP} and θ_{23} , fake CP-violation due to the CC NSIs and the constraints on the source and detector CC NSI parameters at the near and far detectors of DUNE. Since the hierarchy measurements are mainly affected by the NC NSIs [25, 45] in the long baseline experiments like DUNE and the CC NSIs play no important role in the determination of the correct mass ordering, so in our case assuming either mass ordering will not affect our results. For our analysis we consider the normal mass ordering as the true hierarchy.

A. Effects of CC NSIs on simultaneous determination of δ_{CP} and octant of θ_{23} at DUNE

To investigate the effects of source and detector CC NSIs on the determination of δ_{CP} and octant of θ_{23} , we simulate our data by considering two choices of the value of δ_{CP} . First, we take $\delta_{CP} = 0$, which corresponds to the CP-conserving case and second, we consider $\delta_{CP} = 270^\circ$, which is the maximal CP-violation in the standard neutrino oscillation scheme and is determined as the global best fit value [41]. With these two extreme values of δ_{CP} , we find the correlation from the two parameter fits of δ_{CP} vs. θ_{23} in the standard oscillation scheme where we set all of the other NSI parameters equal to zero and minimize over all the other standard oscillation parameters in these fits. In the second case, we repeat the two parameters fit analysis and minimize over both the standard mixing parameters and also over all of the source and detector NSI parameters, $|\varepsilon_{\alpha\beta}|$ and $\phi_{\alpha\beta}$. For minimization over the NSI parameters, we consider the current uncertainty of these parameters from Ref. [19, 43].

Using the characteristics of DUNE and the analysis details as explained in section III, we show the results for the analysis of the simultaneous measurements of θ_{23} and δ_{CP} in Fig. 3. Fig. 3(a) and Fig. 3(b) have been obtained when we minimize only over the standard oscillation parameters while set all NSI parameters equal to zero. On the other

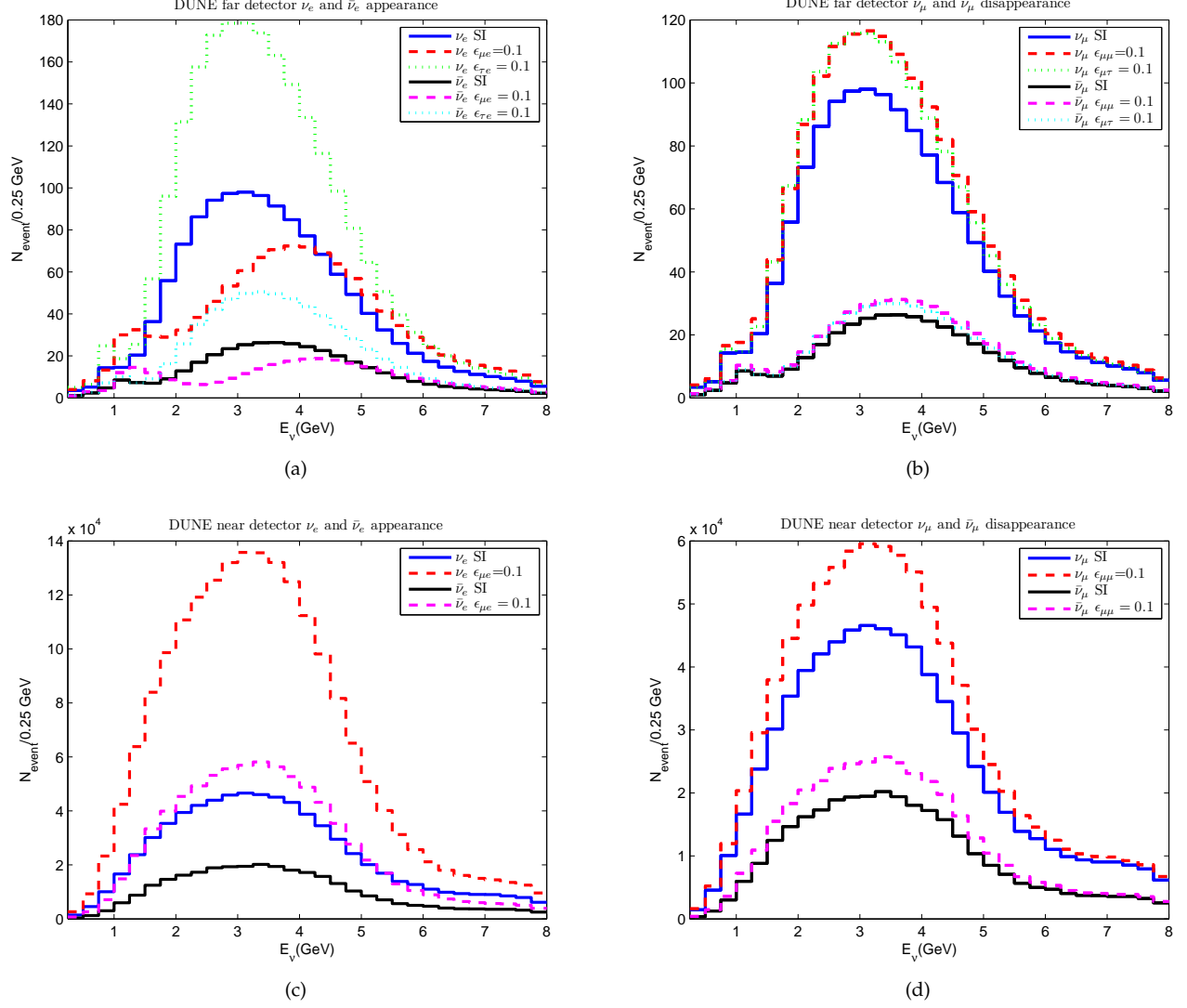


FIG. 2: Number of events per bin for near and far detector of DUNE for three years of data taking in each mode. Number of events includes both signal and background. Oscillation parameters are taken from nu-fit [40, 41]. δ_{CP} is considered equal to zero. Detection efficiencies are taken from Ref. [38] and neutrino flux from Ref. [39]. For NSIs curve, only value of one NSI parameters considered to be nonzero and equal to 0.1. The value of all the phases are set equal to zero.

hand, Fig. 3-c and Fig. 3-d have been obtained when we minimized over both the standard oscillation parameters and over all of the source and detector NSI parameters. Fig. 3(a) and Fig. 3-c correspond to the simulated data with $\delta_{CP} = 0^\circ$, while Fig. 3-b and Fig. 3-d correspond to the $\delta_{CP} = 270^\circ$ case.

By comparing Fig. 3-a with Fig. 3(c) for the $\delta_{CP} = 0^\circ$ and Fig. 3-b with Fig. 3(d) for the $\delta_{CP} = 270^\circ$, the results show that the 3σ C.L. determination of θ_{23} (Fig. 3(a) and Fig. 3(b)) in the standard scenario is destroyed in the presence of CC NSIs (Fig. 3(c) and Fig. 3(d)) within the currently known constraints of the CC NSI parameters from Ref. [19, 43]. When the uncertainties of the source and detector CC NSIs are ignored, the octant of θ_{23} can be determined with 3σ C.L. as shown in Fig. 3(a) and Fig. 3(b), while when these uncertainties are taken into account, the octant cannot be determined with 3σ C.L., and the 2σ and 3σ significance levels get affected due to the CC NSI contributions. Similar deterioration of the 3σ C.L. determination of δ_{CP} within the standard scenario takes place for both types of data when the CC NSIs are included as can be seen by comparing Fig. 3(a) with Fig. 3(c) and Fig. 3(b) with Fig. 3(d). The accuracy of the δ_{CP} measurement gets worsen approximately 80% for $\delta_{CP} = 0^\circ$ and 50% for $\delta_{CP} = 270^\circ$.

B. Effects of the CC NSI fake CP-violation parameter (δ'_{CP})

Due to the importance of δ_{CP} and its explicit measurement program at DUNE we evaluate numerically the impacts of source and detector CC NSI phases ($\phi_{\alpha\beta}$) which can mimic the δ_{CP} measurement resulting into the fake CP-violation (δ'_{CP}), where δ'_{CP} is the measured value of the CP-phase by DUNE which includes the contribution from the standard and nonstandard CP-violating phases. When $\delta_{CP} = 0$, any nonzero measured value of δ'_{CP} could be induced by the nonzero value of NSI parameters, $\varepsilon_{\alpha\beta}$ and $\phi_{\alpha\beta}$. In Fig. 4, we show the one parameter fit of δ'_{CP} results for the various choices of the nonzero values of CC NSI moduli and phases for the special case of $\delta_{CP} = 0^\circ$. We first take the value of $|\varepsilon_{\mu e}|$ and $|\varepsilon_{\tau e}|$ individually as nonzero and then take all the three nonzero at a time, while set them equal to 0.025 in all the cases [19, 43]. In this analysis we consider four values 0° , 90° , 180° and 270° for the corresponding phases in each case. Fig. 4(a) and Fig. 4(b) have been obtained when $|\varepsilon_{\mu e}| = 0.025$ and $|\varepsilon_{\tau e}| = 0.025$, respectively at a time while set the other two parameters equal to zero. The four different choices of the three CC NSI phases are shown through different color legends in the figure. In Fig. 4(c), both absolute parameters $|\varepsilon_{\mu e}|$ and $|\varepsilon_{\tau e}|$ are taken nonzero and set equal to 0.025. Notice that we have minimized over all the standard mixing parameters in this analysis.

The results show that in some cases of the parameter choices, for instance, for black curve of Fig. 4(c), we obtained the best-fit value of δ'_{CP} as 30° more than 80% C.L.. Similarly, in general, we can see from all the three panels of Fig. 4 that the absolute value of δ'_{CP} varies from -50° to 50° . The analysis shows that source and detector CC NSIs parameters can induce a significant amount of fake CP-violations with in the current best limits obtained in Ref. [19, 43].

C. Sensitivities to source and detector CC NSIs at DUNE

We further analyze the simulated data for the DUNE setup to constrain the CC NSI parameters at the source and detector. For this, we simulate our data with all the best fit values of the standard mixing parameters from nu-fit [41] and find the single parameter fits for the relevant absolutes of the NSI parameters while set all the other NSIs parameters to zero. The results of this study are demonstrated in Fig. 5 and the bounds extracted at 90% C.L. are given in table II. We take 90% C.L. projection over the distributions of the single parameter fits to extract the bounds as shown in Fig. 5. We use all the neutrino and antineutrino oscillation channels relevant for DUNE at both the near and far detectors. In the fourth column of table II, we also show the current bounds from the Ref. [43, 44] for comparison. By the general comparison of bounds from this work with the bounds from Ref. [43, 44] (fourth column of table II) shows that for the 3+3 years of running, DUNE has a potential to give more stringent bounds than the existing ones from the other experiments [18, 19]. Interestingly, the bounds for the relevant parameters at the near detector has an overall one order of magnitude improvement than all of the current bounds, while using the data of the far detector, there is an overall a factor of 2 improvement except for $\varepsilon_{\mu\tau}$, $\varepsilon_{\tau e}$ and $\varepsilon_{\tau\mu}$ parameters which are weakly constrained in comparison to the current bounds.

As discussed in section II, the near detector is sensitive to ε_{ee} , $\varepsilon_{\mu\mu}$ and $\varepsilon_{\mu e}$, but not to $\varepsilon_{\mu\tau}$, $\varepsilon_{e\mu}$, $\varepsilon_{\tau\mu}$ and $\varepsilon_{\tau e}$, thus the former set of parameter can be constrained at the near detector as shown in Fig.5(a, b, c), while the latter cannot be constrained as can be seen in Fig.5(d, e, f, g). As can be seen from TABLE II, constraints on $\varepsilon_{\mu\tau}$, $\varepsilon_{e\mu}$, $\varepsilon_{\tau e}$, $\varepsilon_{\tau\mu}$ at the far detector are stronger in some cases while weaker in the others. For the far detector, when we fix δ_{CP} or θ_{23} to their central values and try to find correlation between the NSI parameters $\varepsilon_{\mu\tau}$, $\varepsilon_{e\mu}$, $\varepsilon_{\tau e}$, $\varepsilon_{\tau\mu}$ and δ_{CP} or θ_{23} , we find that there is a strong correlation between $\varepsilon_{\tau e}$ and δ_{CP} and the constraint on this parameter at 90% C.L. is 0.042. The same correlation, although weaker, also exists for $\varepsilon_{e\mu}$. Similar correlations also exist between $\varepsilon_{\mu\tau}$, $\varepsilon_{\tau\mu}$ and θ_{23} , where the bounds at the 90% C.L. are 0.013 and 0.014, respectively. This indicates that the weaker bounds of some of the parameters are due to the existing uncertainties in δ_{CP} and θ_{23} .

As a check we also repeat the exercise of the analysis of Fig. 3 using the bounds obtained from this study for the near detector case and found that there are marginal differences from the results of Fig. 3. The reason is that the near detector cannot constrain the $\varepsilon_{\tau e}$ parameter and, as shown in the subsection A above, this parameter is central to the appearance channels and has a large impact on the measurement of δ_{CP} and octant of θ_{23} . Notice that the near detector will constrain $\varepsilon_{\mu e}$. If these parameters have values $O(0.01)$, their effects will be detectable in the near detector. Since the near detector is sensitive to $\varepsilon_{\mu e}$, the near detector can be more helpful to discriminate between δ'_{CP} and δ_{CP} than the far detector. Also near detector has no sensitivity to $\varepsilon_{\tau e}$, so it cannot discriminate between δ'_{CP} and δ_{CP} in all the cases. We do similar simulations for Fig. 4 with the near detector bounds obtained in this work, and in case similar to Fig.4(a) the induced fake CP phase is negligible, $\delta'_{CP} = 0$. In the case similar to Fig.4(b), since the near detector do not constrain $\varepsilon_{\tau e}$, the result is the same as Fig.4(b), and in the case of Fig.4(c), the effect of induced fake

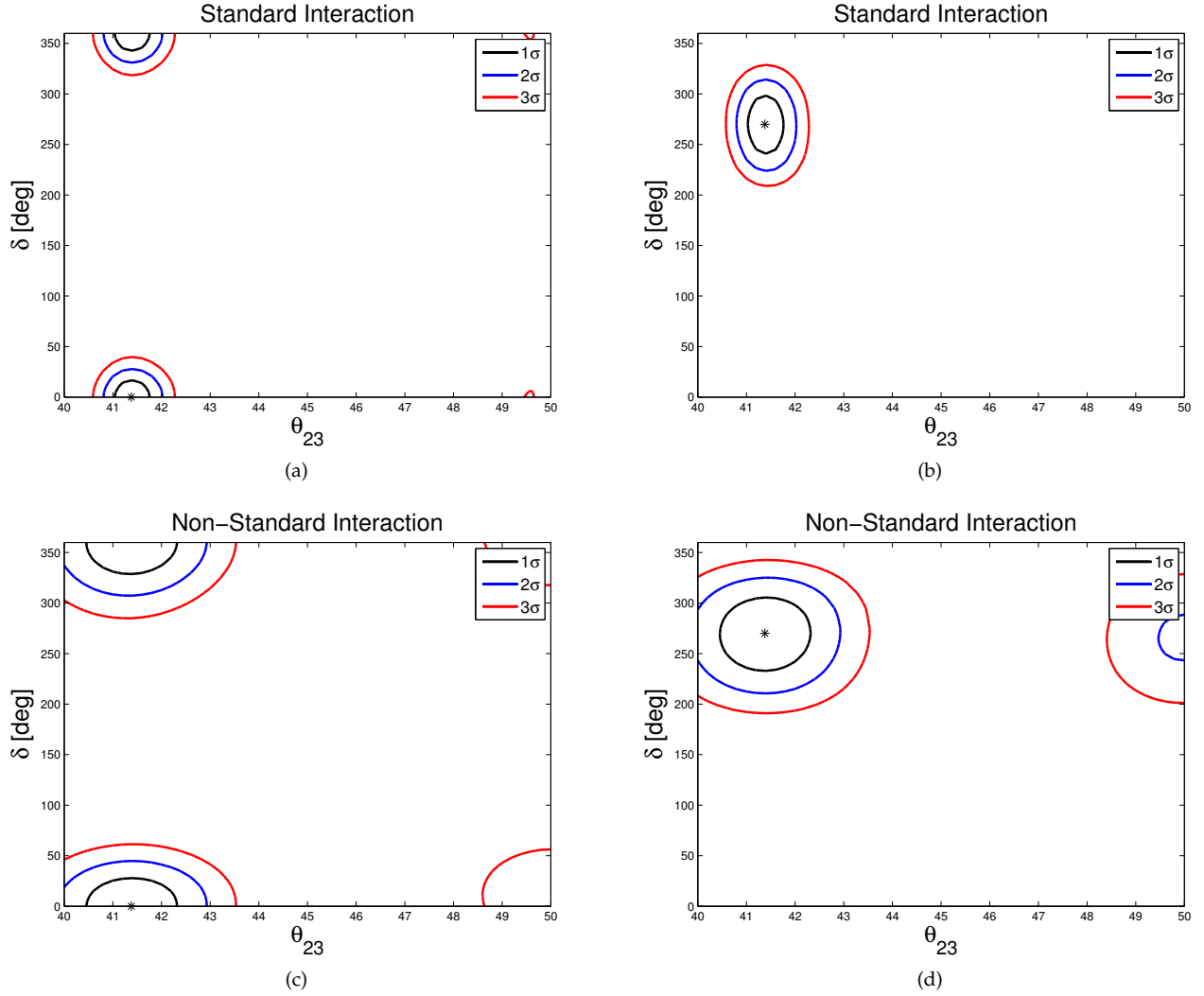


FIG. 3: Simultaneous determination of δ_{CP} and octant of θ_{23} by DUNE after six years of data taking, three years in each mode, for $\delta_{CP} = 0^\circ$ for panels a and c and $\delta_{CP} = 270^\circ$ for panels b and d. In panels a and b, we marginalized over the standard oscillation parameters, while in panels c and d, we marginalized over standard and NSI source and detector parameters.

CP phase is less than half of the result demonstrated in Fig.4(c).

V. SUMMARY AND CONCLUSIONS

In this paper, we have explored the effects of CC NSIs at DUNE. We have studied the impacts on the simultaneous measurements of the δ_{CP} and θ_{23} due to the CC NSIs at neutrino source and at the detector. We study how the statistical significance level of the measurement of δ_{CP} and θ_{23} at the same time gets affected by the CC NSI inputs. We also checked how the NSI parameters can induce a fake CP-violation (δ'_{CP}) effects, when the standard δ_{CP} is set to zero in the NSI model. Further, we find constraints on the CC NSIs at the source and detector for the simulated data of DUNE.

As discussed in section IV and demonstrated in Fig. 3, we take two choices to see the impact of CC NSIs on the simultaneous measurements of δ_{CP} and θ_{23} . First, we have minimized over the NSI parameters as shown in Fig. 3-c and Fig. 3-d, while in the second case we did not marginalize over the NSIs parameters and this is shown in Fig. 3-a and Fig. 3-b. The results demonstrate that in the absence of CC NSIs, the octant of θ_{23} can be determined at 3σ C.L., while in the presence of the CC NSIs, the octant cannot be determined at 3σ C.L. Similarly, the CC NSIs also affect the determination of δ_{CP} and its measurement gets worsen by approximately 80% and 50% in the two cases of

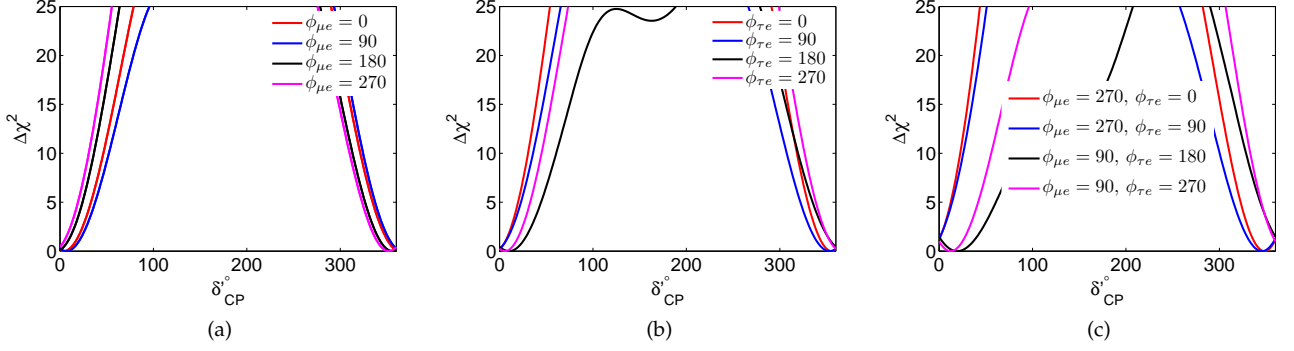


FIG. 4: Induced fake CP-violation phase δ'_{CP} in DUNE by considering nonzero source and detector NSIs. In panels a and b only $|\epsilon_{\mu e}|$ and $|\epsilon_{\tau e}|$ is nonzero and is set equal to 0.025 respectively and the values of corresponding NSI phases are 0° , 90° , 180° and 270° . All the other NSI parameters are set equal to zero. In panel c all of these NSI parameters are considered nonzero and equal to 0.025. The values of corresponding NSI phases are shown in the legends.

Parameters	Far Detector	Near Detector	Current Constraints
$ \epsilon_{ee} $	0.046	0.003	0.041
$ \epsilon_{\mu\mu} $	0.015	0.002	0.078
$ \epsilon_{\mu e} $	0.009	0.006	0.026
$ \epsilon_{\mu\tau} $	0.074	-	0.013
$ \epsilon_{e\mu} $	0.049	-	0.026
$ \epsilon_{\tau\mu} $	0.076	-	0.013
$ \epsilon_{\tau e} $	0.113	-	0.041

TABLE II: One degree of freedom constraints on the CC NSI parameters at the near and far detector of DUNE, obtained from Fig. 5 at 90% C.L., while the current “indirect” bounds from Ref. [43, 44] at 90% C.L. also given in fourth row for comparison. The blank entries indicate that the DUNE near detector has no sensitivity to these parameters.

different data.

We investigated the effects of NSIs to induce fake CP-violation through the parameter δ'_{CP} . The results of Fig. 4 show that in some cases δ'_{CP} can be large ($\delta'_{CP} \sim 30^\circ$), and $\delta'_{CP} \sim 0^\circ$ can be excluded by more than 80% C.L. With these results, we can conclude that the effect of source and detector CC NSIs are important in determining δ_{CP} and the CC NSIs can induce large amount of fake CP-violation. We showed the near detector of DUNE can help to constrain the source and detector CC NSIs and distinguish between δ'_{CP} and δ_{CP} .

The results on constraining all of the relevant NSI parameters in this study at the near and far detectors data of DUNE are displayed in Fig. 5. The related bounds obtained at 90% C.L. from the one parameter-at-a-time fits of Fig. 5 are given in Table I. The results show that DUNE near detector has a stronger potential to constrain the CC NSIs more tightly, better than one order of magnitude in comparison to the existing bounds on the CC NSI parameters at the source and at the detector. The bounds obtained from the simulated data of the far detector can also improved by one order of magnitude for some parameters but remain weaker for the others.

Acknowledgments

Authors are grateful to Y. Farzan and D. McKay for useful comments and careful reading of the manuscript. P.B. acknowledges partial support from the European Unions Horizon 2020 research and innovation programme under the Marie Skłodowska-Curie grant agreement No. 674896 and No. 690575. A. K. work has been financially supported by the Sun Yat-Sen University under the Post-Doctoral Fellowship program and the China Postdoctoral

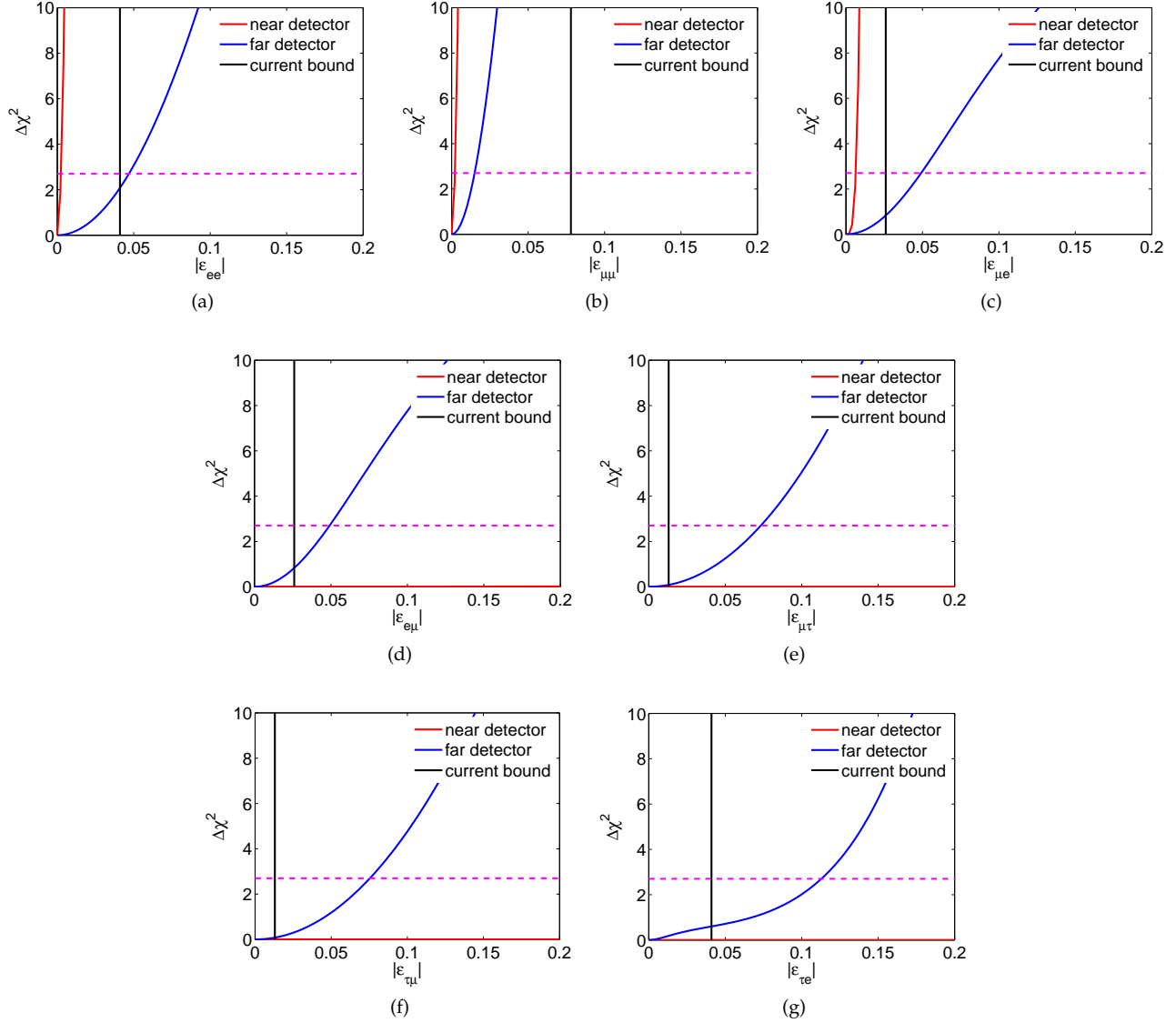


FIG. 5: Constraints on source and detector NSI parameters by near and far detector of DUNE. The current “indirect” bounds at the 90% C.L. from Ref. [43] for each parameter are shown by the black lines for comparison. The 90% C.L. projections are shown by dashed lines.

Science Foundation under the grant # 74130-41090002.

-
- [1] K. Abe *et al.* [T2K Collaboration], Indication of Electron Neutrino Appearance from an Accelerator-produced Off-axis Muon Neutrino Beam, *Phys. Rev. Lett.* **107** (2011) 041801, arXiv:1106.2822.
 - [2] Y. Abe *et al.* (Double Chooz Collaboration), Indication for the disappearance of reactor electron antineutrinos in the Double Chooz experiment, *Phys. Rev. Lett.* **108**, 131801 (2012), , arXiv:1112.6353; Reactor electron antineutrino disappearance in the Double Chooz experiment, *Phys. Rev. D* **86**, 052008 (2012), arXiv:1207.6632.
 - [3] J. K. Ahn *et al.* (RENO Collaboration), Observation of Reactor Electron Antineutrino Disappearance in the RENO Experiment, *Phys. Rev. Lett.* **108**, 191802 (2012), arXiv: 1204.0626.
 - [4] F. An *et al.* (Daya Bay Collaboration), Observation of electron-antineutrino disappearance at Daya Bay, *Phys. Rev. Lett.* **108**, 171803 (2012), arXiv: 1203.1669; Improved Measurement of Electron Antineutrino Disappearance at Daya Bay, *Chin. Phys. C* **37**, 011001(2013), arXiv:1210.6327.

- [5] Y.-F. Li, Overview of the Jiangmen Underground Neutrino Detector (JUNO), arXiv:1402.6143v1.
- [6] S. Seo, Introduction to RENO-50, in Proceedings of the International Workshop on RENO-50: Toward Neutrino Mass Hierarchy, Seoul, 2013.
- [7] K. Abe *et al.* [T2K Collaboration], Neutrino oscillation physics potential of the T2K experiment, PTEP **2015** (2015) no.4, 043C01, arXiv:1409.7469.
- [8] P. Adamson *et al.* [NOvA Collaboration], First measurement of muon-neutrino disappearance in NOvA, Phys. Rev. D **93** (2016) no.5, 051104 arXiv:1601.05037.
- [9] K. Abe *et al.* [Hyper-Kamiokande Proto- Collaboration], Physics potential of a long-baseline neutrino oscillation experiment using a J-PARC neutrino beam and Hyper-Kamiokande, PTEP **2015** (2015) 053C02, arXiv:1502.05199.
- [10] R. Acciarri *et al.* [DUNE Collaboration], Long-Baseline Neutrino Facility (LBNF) and Deep Underground Neutrino Experiment (DUNE) Conceptual Design Report Volume 2: The Physics Program for DUNE at LBNF, arXiv:1512.06148; C. Adams *et al.* [LBNE Collaboration], The Long-Baseline Neutrino Experiment: Exploring Fundamental Symmetries of the Universe, arXiv:1307.7335.
- [11] H. Minakata and S. J. Parke, Correlated, precision measurements of θ_{13} and δ using only the electron neutrino appearance experiments, Phys. Rev. D **87** (2013) no.11, 113005, arXiv:1303.6178.
- [12] K. Abe *et al.*, Letter of Intent: The Hyper-Kamiokande Experiment — Detector Design and Physics Potential —, arXiv:1109.3262.
- [13] C. Adams *et al.* (LBNE Collaboration), arXiv:1307.7335
- [14] IDS-NF Collaboration, International Design Study for a Neutrino Factory, <https://www.ids-nf.org/wiki/FrontPage>.
- [15] E. Baussan *et al.* (ESSnuSB Collaboration), Nucl. Phys. B **885**, 127 (2014).
- [16] P. Coloma, H. Minakata and S. J. Parke, Interplay between appearance and disappearance channels for precision measurements of θ_{13} and δ , Phys. Rev. D **90** (2014) 093003, arXiv:1406.2551.
- [17] A. N. Khan, D. W. McKay and F. Tahir, Sensitivity of medium-baseline reactor neutrino mass-hierarchy experiments to nonstandard interactions, Phys. Rev. D **88**, 113006 (2013), arXiv:1305.4350.
- [18] A. N. Khan, D. W. McKay and F. Tahir, Short baseline $\bar{\nu} - e$ reactor scattering experiments and nonstandard neutrino interactions at source and detector Phys.Rev. D **90**, 053008 (2014), arXiv:1407.4263.
- [19] A. N. Khan, Global analysis of the source and detector nonstandard interactions using the short baseline $\nu - e$ and $\bar{\nu} - e$ scattering data, Phys. Rev. D **93** (2016) no.9, 093019, arXiv:1605.09284.
- [20] I. Girardi, D. Meloni and S. T. Petcov, The Daya Bay and T2K results on $\sin^2 2\theta_{13}$ and Non-Standard Neutrino Interactions, Nucl. Phys. B **886** (2014) 31, arXiv:1405.0416.
- [21] I. Girardi and D. Meloni, Constraining new physics scenarios in neutrino oscillations from Daya Bay data, Phys. Rev. D **90** (2014) no.7, 073011, arXiv:1403.5507.
- [22] A. de Gouvea and K. J. Kelly, Non-standard Neutrino Interactions at DUNE, Nucl. Phys. B **908** (2016) 318, arXiv:1511.05562.
- [23] J. Liao, D. Marfatia and K. Whisnant, Degeneracies in long-baseline neutrino experiments from nonstandard interactions, arXiv:1601.00927.
- [24] P. Coloma, Non-Standard Interactions in propagation at the Deep Underground Neutrino Experiment, JHEP **1603**, 016 (2016), arXiv:1511.06357.
- [25] P. Coloma and T. Schwetz, Generalized mass ordering degeneracy in neutrino oscillation experiments, arXiv:1604.05772.
- [26] M. Masud and P. Mehta, Non-standard interactions and the resolution of ordering of neutrino masses at DUNE and other long baseline experiments, arXiv:1606.05662.
- [27] M. Blennow, S. Choubey, T. Ohlsson, D. Pramanik and S. K. Raut, A combined study of source, detector and matter non-standard neutrino interactions at DUNE, arXiv:1606.08851.
- [28] P. Bakhti and Y. Farzan, CP-Violation and Non-Standard Interactions at the MOMENT, arXiv:1602.07099.
- [29] J. Cao *et al.*, Muon-decay medium-baseline neutrino beam facility, Phys. Rev. ST Accel. Beams **17** (2014) 090101, arXiv:1401.8125.
- [30] S. K. Agarwalla, P. Bagchi, D. V. Forero and M. Tortola, JHEP **1507** (2015) 060, arXiv:1412.1064.
- [31] D. Dutta, R. Gandhi, B. Kayser, M. Masud and S. Prakash, JHEP **1611** (2016) 122, arXiv:1607.02152.
- [32] S. K. Agarwalla, S. S. Chatterjee and A. Palazzo, Phys. Lett. B **762** (2016) 64, arXiv:1607.01745.
- [33] F. J. Escrivuela, D. V. Forero, O. G. Miranda, M. Tortola and J. W. F. Valle, arXiv:1612.07377.
- [34] T. Ohlsson, Status of non-standard neutrino interactions, Rept. Prog. Phys. **76** (2013) 044201, arXiv:1209.2710.
- [35] M. Blennow, S. Choubey, T. Ohlsson and S. K. Raut, Exploring Source and Detector Non-Standard Neutrino Interactions at ESSnuSB, JHEP **1509** (2015) 096, arXiv:1507.02868.
- [36] J. Kopp, M. Lindner, T. Ota and J. Sato, Non-standard neutrino interactions in reactor and superbeam experiments, Phys. Rev. D **77** (2008) 013007, arXiv:0708.0152.
- [37] J. Kopp, Efficient numerical diagonalization of hermitian 3×3 matrices, Int. J. Mod. Phys. C **19** (2008) 523, arXiv:physics/0610206.
- [38] C. Adams *et al.* [LBNE Collaboration], The Long-Baseline Neutrino Experiment: Exploring Fundamental Symmetries of the Universe, arXiv:1307.7335 [hep-ex].
- [39] <http://home.fnal.gov/~ljf26/DUNE2015CDRFluxes/>
- [40] M. C. Gonzalez-Garcia, M. Maltoni, J. Salvado and T. Schwetz, Global fit to three neutrino mixing: critical look at present precision, JHEP **1212**, 123 (2012), arXiv:1209.3023.
- [41] M. C. Gonzalez-Garcia, M. Maltoni and T. Schwetz, Updated fit to three neutrino mixing: status of leptonic CP violation, JHEP **1411**, 052 (2014), arXiv:1409.5439.

- [42] S. Choubey and D. Pramanik, Constraints on Sterile Neutrino Oscillations using DUNE Near Detector, arXiv:1604.04731 [hep-ph].
- [43] C. Biggio, M. Blennow and E. Fernandez-Martinez, General bounds on non-standard neutrino interactions, JHEP **0908**, 090 (2009), arXiv:0907.0097.
- [44] O.G. Miranda and H. Nunokawa, New J. Phys. **17**, no. 9, 095002 (2015), arXiv:1505.06254.
- [45] P. Bakhti and Y. Farzan, Shedding light on LMA-Dark solar neutrino solution by medium baseline reactor experiments: JUNO and RENO-50, JHEP **1407**, 064 (2014), arXiv:1403.0744.
- [46] A. M. Dziewonski and D. L. Anderson, Geophysical aspects of very long baseline neutrino experiments, Phys. Earth Planet. Interiors **25** (1981) 297; R. J. Geller and T. Hara, Nucl. Instrum. Meth. A **503** (2003) 187, arXiv: hep-ph/0111342.
- [47] P. Huber, M. Lindner and W. Winter, Simulation of long-baseline neutrino oscillation experiments with GLoBES (General Long Baseline Experiment Simulator), Comput. Phys. Commun. **167** (2005) 195, arXiv: hep-ph/0407333.
- [48] P. Huber, J. Kopp, M. Lindner, M. Rolinec and W. Winter, New features in the simulation of neutrino oscillation experiments with GLoBES 3.0: General Long Baseline Experiment Simulator, Comput. Phys. Commun. **177** (2007) 432, arXiv: hep-ph/0701187.
- [49] M. D. Messier, Evidence for neutrino mass from observations of atmospheric neutrinos with Super-Kamiokande, UMI-99-23965.
- [50] E. A. Paschos and J. Y. Yu, Neutrino interactions in oscillation experiments, Phys. Rev. D **65**, 033002 (2002), arXiv: hep-ph/0107261.
- [51] R. Acciarri *et al.* [DUNE Collaboration], Long-Baseline Neutrino Facility (LBNF) and Deep Underground Neutrino Experiment (DUNE) : Volume 1: The LBNF and DUNE Projects, arXiv:1601.05471.
- [52] J. M. Berryman, A. de Gouvea, K. J. Kelly and A. Kobach, Sterile neutrino at the Deep Underground Neutrino Experiment, Phys. Rev. D **92** (2015) no.7, 073012, arXiv:1507.03986.